Regulation of the inflammatory synovial fibroblast phenotype by metastasis-associated lung adenocarcinoma transcript 1 long noncoding RNA in obese patients with osteoarthritis

Nanus, Dominika; Wijesinghe, Susanne; Pearson, Mark; Hadjicharalambous, Marina; Rosser, Alex; Davis, Edward; Lindsay, Mark; Jones, Simon

DOI:
10.1002/art.41158

Document Version
Publisher's PDF, also known as Version of record

Citation for published version (Harvard):
Nanus, D, Wijesinghe, S, Pearson, M, Hadjicharalambous, M, Rosser, A, Davis, E, Lindsay, M & Jones, S 2020, 'Regulation of the inflammatory synovial fibroblast phenotype by metastasis-associated lung adenocarcinoma transcript 1 long noncoding RNA in obese patients with osteoarthritis', *Arthritis and Rheumatology*, vol. 72, no. 4, pp. 609-619. https://doi.org/10.1002/art.41158

Arthritis & Rheumatology
Vol. 72, No. 4, April 2020, pp 609–619
DOI 10.1002/art.41158

American College of Rheumatology
Empowering Rheumatology Professionals

Regulation of the Inflammatory Synovial Fibroblast Phenotype by Metastasis-Associated Lung Adenocarcinoma Transcript 1 Long Noncoding RNA in Obese Patients With Osteoarthritis

Dominika E. Nanus,[1] Susanne N. Wijesinghe,[1] Mark J. Pearson,[1] Marina R. Hadjicharalambous,[2] Alex Rosser,[1] Edward T. Davis,[3] Mark A. Lindsay,[4] and Simon W. Jones[1]

Objective. To identify long noncoding RNAs (lncRNAs) associated with the inflammatory phenotype of synovial fibroblasts from obese patients with osteoarthritis (OA), and to explore the expression and function of these lncRNAs.

Methods. Synovium was collected from normal-weight patients with hip fracture (non-OA; n = 6) and from normal-weight (n = 8) and obese (n = 8) patients with hip OA. Expression of RNA was determined by RNA-sequencing and quantitative reverse transcription–polymerase chain reaction. Knockdown of lncRNA was performed using LNA-based GapmeRs. Synovial fibroblast cytokine production was measured by enzyme-linked immunosorbent assay.

Results. Synovial fibroblasts from obese patients with OA secreted greater levels of interleukin-6 (IL-6) (mean ± SEM 162 ± 21 pg/ml; $P < 0.001$) and CXCL8 (262 ± 67 pg/ml; $P < 0.05$) compared to fibroblasts from normal-weight patients with OA (IL-6, 51 ± 4 pg/ml; CXCL8, 78 ± 11 pg/ml) or non-OA patients (IL-6, 35 ± 3 pg/ml; CXCL8, 56 ± 6 pg/ml) (n = 6 patients per group). RNA-sequencing revealed that fibroblasts from obese OA patients exhibited an inflammatory transcriptome, with increased expression of proinflammatory messenger RNAs (mRNAs) as compared to that in fibroblasts from normal-weight OA or non-OA patients (>2-fold change, $P < 0.05$; n = 4 patients per group). A total of 19 lncRNAs were differentially expressed between normal-weight OA and non-OA patient fibroblasts, and a further 19 lncRNAs were differentially expressed in fibroblasts from obese OA patients compared to normal-weight OA patients (>2-fold change, $P < 0.05$ for each), which included the lncRNA for metastasis-associated lung adenocarcinoma transcript 1 (MALAT1). MALAT1 was rapidly induced upon stimulation of OA synovial fibroblasts with proinflammatory cytokines, and was up-regulated in the synovium from obese OA patients as compared to normal-weight OA patients (1.6-fold change, $P < 0.001$) or non-OA patients (6-fold change, $P < 0.001$). MALAT1 knockdown in OA synovial fibroblasts (n = 4 patients) decreased the levels of mRNA expression and protein secretion of CXCL8 (>1.5-fold change, $P < 0.01$), whereas it increased expression of mRNAs for TRIM6 (>2-fold change, $P < 0.01$), IL7R (<2-fold change, $P < 0.01$), HIST1H1C (>1.5-fold change, $P < 0.001$), and MAML3 (>1.5-fold change, $P < 0.001$). In addition, MALAT1 knockdown inhibited the proliferation of synovial fibroblasts from obese patients with OA.

Conclusion. Synovial fibroblasts from obese patients with hip OA exhibit an inflammatory phenotype. MALAT1 lncRNA may mediate joint inflammation in obese OA patients.

INTRODUCTION

Osteoarthritis (OA) has historically been considered a wear-and-tear disease of the articular cartilage. In contrast to rheumatoid arthritis (RA), in which synovial inflammation (synovitis) is an active driver of disease (1) and targeting of synovial fluid proinflammatory cytokines is the rationale behind many of the existing RA therapeutics, OA is often referred to as a noninflammatory joint disease. As

Supported by Arthritis Research UK (grants 21530 and 21812). Dr. Lindsay's work was supported by the Biotechnology and Biological Sciences Research Council (grant BB/K00623/1).

[1]Dominika E. Nanus, PhD, Susanne N. Wijesinghe, PhD, Mark J. Pearson, PhD, Alex Rosser, MSc, Simon W. Jones, PhD: University of Birmingham, Birmingham, UK; [2]Marina R. Hadjicharalambous, PhD: University of Bath, Bath, UK; [3]Edward T. Davis, MbChB: Royal Orthopaedic Hospital, Birmingham, UK; [4]Mark A. Lindsay, PhD: University of Birmingham, Birmingham, UK, and University of Bath, Bath, UK.

Drs. Nanus and Wijesinghe contributed equally to this work. Drs. Lindsay and Jones contributed equally to this work.

No potential conflicts of interest relevant to this article were reported.

Address correspondence to Simon W. Jones, PhD, Institute of Inflammation and Ageing, University of Birmingham, MRC-ARUK Centre for Musculoskeletal Ageing Research, Edgbaston, Birmingham B15 2TT, UK. E-mail: s.w.jones@bham.ac.uk.

Submitted for publication January 7, 2019; accepted in revised form October 31, 2019.

such, OA drug development has predominantly focused on directly targeting the catabolic and anabolic pathways of cartilage tissue, which has been of limited success (2). However, increasing evidence indicates that synovitis plays a significant role in OA joint pathology (2–4) by exacerbating cartilage damage via the induction of matrix metalloproteases and aggrecanases (5–7), and by hastening the onset of end-stage disease. Magnetic resonance imaging and histologic analyses have shown that synovitis is present at all stages of OA pathogenesis (8–10), with hyperplasia of the synovial lining (11,12), infiltration of immune cells (13,14), and expression of proinflammatory cytokines (15–17). The presence of synovitis in early OA, in patients who have minimal radiographic signs of cartilage loss (11), suggests that the emergence of synovitis may represent an opportune point for early therapeutic intervention (3).

We recently reported that the synovial fluid in OA patients who are obese contains greater levels of interleukin-6 (IL-6), tumor necrosis factor (TNF), and CXCL8, as compared to the synovial fluid in normal-weight OA patients, and that isolated synovial fibroblasts from obese OA patients secrete more IL-6 (15). Obesity may therefore drive synovial fibroblasts to adopt a more inflammatory phenotype, thereby contributing to an inflammatory environment in the joint to which the cartilage is exposed. As such, synovitis may play a particularly significant role in the onset and progression of OA in obese individuals, with implications for patient stratification in clinical testing of antiinflammatory therapeutics (3). Furthermore, determining how obesity-associated inflammation within the synovial joint tissue is regulated may lead to the development of new antiinflammatory therapies, which could be of benefit to patients diagnosed as having OA and might help prevent the onset of disease in "at-risk" obese patient populations.

In attempting to better understand the cellular regulators of synovial joint inflammation, investigators have identified long noncoding RNAs (lncRNAs) (18,19) as a central regulator of the inflammatory response (20–24). We recently identified lncRNAs that are associated with the inflammatory response in human OA chondrocytes, which function by regulating the secretion of proinflammatory cytokines (22,25). Therefore, the aim of the present study was to characterize the transcriptome of synovial fibroblasts isolated from either obese or normal-weight patients with hip OA, as well as synovial fibroblasts from normal-weight patients with hip fracture (non-OA), in analyses using RNA-sequencing (RNA-seq) to identify lncRNAs associated with the inflammatory synovial fibroblast phenotype, and to examine the expression and functional role of metastasis-associated lung adenocarcinoma transcript 1 (MALAT1), a differentially expressed lncRNA in OA synovium.

PATIENTS AND METHODS

Patients and tissue samples. Obese and normal-weight patients with hip OA and normal-weight patients with femoral neck fracture (non-OA patients) who were scheduled to undergo elective arthroplasty were recruited for the study. Ethics approval was provided by the UK National Research Ethics Committee (approval no. 14/ES/1044), and informed consent was obtained from all patients. The characteristics of the study patients are shown in Table 1.

Synovium was collected perioperatively. A portion of synovium was snap-frozen in liquid nitrogen and pulverized for analysis of RNA expression. The remaining synovium was used for isolation of primary synovial fibroblasts.

Isolation and culture of primary fibroblasts from synovium. Synovial membrane was diced (~1 mm^3) and cultured in growth medium (RPMI 1640 containing 10% fetal calf serum [FCS], 1% penicillin–streptomycin, 5% L-glutamine, 5% sodium pyruvate, and 5% nonessential amino acids [Sigma-Aldrich]).

Table 1. Characteristics of the study patients*

	Obese OA (n = 8)	Normal-weight OA (n = 8)	Non-OA (n = 6)
Demographic			
Age, years	65.1 ± 4.6	65.5 ± 2.3	69.7 ± 2.9
Female/male, %	50/50	50/50	50/50
Anthropometric			
BMI, kg/m^2	39.8 ± 3.6	23.3 ± 0.3†	22.9 ± 0.6†
Waist circumference, cm	92 ± 18.6	75 ± 8.1	–
Hip circumference, cm	100 ± 21.9	88 ± 6.4	–
WHR	0.93 ± 0.02	0.82 ± 0.05	–
OA severity measure			
Joint space width, mm	1.1 ± 1.1	0.94 ± 0.6	–
K/L radiographic grade			
Median (IQR)	4 (3.3–4)	4 (3.3–4)	–
Grade I, %	0	0	–
Grade II, %	12.5	12.5	–
Grade III, %	12.5	12.5	–
Grade IV, %	75	75	–

* Except where indicated otherwise, values are the mean ± SEM. BMI = body mass index; WHR = waist:hip circumference ratio; K/L= Kellgren/Lawrence; IQR = interquartile range.
† $P < 0.0001$ versus obese patients with osteoarthritis (OA).

Synovial fibroblasts were grown to 70-80% confluence, and phenotype was confirmed by identification of CD55-positive cells, as described previously (15).

RNA-seq analysis. Synovial fibroblasts were cultured for 24 hours in culture medium containing 0.1% FCS, without antibiotics. Total RNA was isolated using TRIzol (Life Technologies) and purified using an RNeasy column (Qiagen). RNA integrity number (RIN) values (Agilent Bioanalyzer) were >7. Paired-end and stranded 75-bp sequencing data were obtained using an Illumina HiSeq4000, carried out at the Oxford Genomics Centre (Wellcome Centre for Human Genetics, UK).

For the analysis of fibroblasts following knockdown of MALAT1 lncRNA, RNA-seq was performed using a QuantSeq 3′ kit (Lexogen). Sequencing data were analyzed as previously described (25). Briefly, the paired-end reads were aligned to the human reference genome (hg38) using Hisat2 (version 2.0.4) (26) with the following command line options: hisat2 -q --dta --rna-strandness FR –x <reference-genone.gtf> -1 <forward_strand.fa> -2 <reverse-strand file.fa> –S <output.sam>. Using Samtools (27), output SAM files were sorted and converted to BAM files (Samtools command line sort -@ 8 –o output.bam output.sam) and indexed (Samtools command line index –b output.bam). The profile of gene expression (using the Gencode version 27 database and additional novel lncRNAs) (25) in the BAM files for each sample were determined using Stringtie (26,28), with the following command line: stringtie <sample.BAM> -G <GenCodev26.gtf> -o <samples.gtf> -e -A <sample.txt>. The differential expression of genes derived from Gencode version 27 and our recently generated list of novel lncRNAs implicated in the innate immune system (25) was assessed with the geometric option in Cuffdiff version 2.2.1.3 (part of the Cufflinks suite) (29), applying a significance threshold of $q < 0.05$. The command line options were as follows: cuffdiff –FDR=0.05 --min-alignment-count=10--library-norm-method=geometric--dispersion-method=pooled -u <reference_genome.gtf> <control_1.bam>, <control_x.bam> <activated_1.bam>,<activated_x.bam> -o <output_file_name>.

Principal components analysis (PCA) and hierarchical clustering. The abundance of Gencode version 27–defined genes in individual samples was defined as the fragments per kilobase exon per million reads mapped (FPKM) and determined using Stringtie (RNA) as described above. PCA and hierarchical clustering on Gencode version 27 protein–coding genes that demonstrated an expression value of >1 FPKM was performed using Genesis (version 1.7.7) (30). Data were $\log_2$-transformed following the addition of 1 FPKM. The threshold for reporting gene expression at FPKM >1 is based on the ability to validate sequencing data using quantitative reverse transcription–polymerase chain reaction (qRT-PCR) (31). RNA-seq data can be obtained from the Gene Expression Omnibus database (at http://www.ncbi.nlm.nih.gov/geo/).

Pathway analysis. Differentially expressed genes (defined as those with >1.5-fold change in expression; $P < 0.05$) were identified using DAVID and Ingenuity Pathway Analysis (IPA) software (online at https://www.ingenuity.com). In the DAVID analysis tool (https://david.ncifcrf.gov), genes were analyzed using the KEGG pathway option. Using IPA software, a core functional analysis was performed to identify canonical pathways and predicted upstream regulators that were significantly associated with the differentially expressed messenger RNAs (mRNAs). The significance of the association of a given canonical pathway with the differentially expressed mRNAs was measured based on the ratio of the number of mapped differentially expressed mRNAs in the data set divided by the total number of genes that map to the canonical pathway, with *P* values calculated using Fisher's exact test for the association between each mRNA and the canonical pathway. For the prediction of upstream regulators, *P* values and Z scores were computed based on the significant overlap between genes in the data set and known targets regulated by the transcriptional regulator.

Quantitative RT-PCR. Primers for individual transcripts (see Supplementary Table 1, available on the *Arthritis & Rheumatology* web site at http://onlinelibrary.wiley.com/doi/10.1002/art.41158/abstract) were designed using Primer Express 3 software (Life Technologies). PCR was performed from total RNA in a 1-step reaction (iTaq Universal One-Step; BioRad). Relative expression was determined using the $\Delta\Delta C_t$ method, followed by normalization of values to those for 18S.

Inhibition of lncRNA expression using LNA GapmeRs. Primary synovial fibroblasts (obtained from 4 patients) were transfected with 2 different LNA GapmeR inhibitors (Exiqon) targeting MALAT1 lncRNA (30 n*M*) or with a control LNA inhibitor (30 n*M*), using Lipofectamine 3000 (Invitrogen). After 24 hours, the supernatants were collected for cytokine analysis by enzyme-linked immunosorbent assay (ELISA), and cells were lysed with RLT buffer (Qiagen) for RNA extraction. All RIN values (Agilent Bioanalyzer) were >8. RNA was analyzed by qRT-PCR and RNA-seq analyses (QuantSeq 3′; Lexogen). RNA-seq data were analyzed using Cuffdiff to identify differentially expressed genes.

Determination of synovial fibroblast proliferation. Proliferation of synovial fibroblasts was determined using a CellTiter 96 Aqueous One Solution Cell Proliferation Assay kit (Promega) in accordance with the manufacturer's instructions. Briefly, cells were cultured in 96-well plates and, following the addition of MTS reagent, the absorbance at 490 nm was measured using a microplate reader (SynergyHT; BioTek).

Statistical analysis. Data were analyzed using GraphPad Prism 6 software. Groups were compared by one-way analysis of variance with Dunnett's test for multiple comparisons. Data are

presented as the mean ± SEM, with *P* values less than 0.05 defining statistically significant differences.

RESULTS

Inflammatory phenotype of synovial fibroblasts isolated from obese OA patients. Synovial fibroblasts from normal-weight non-OA patients, normal-weight OA patients, and obese OA patients (n = 6 patients per group) were cultured for 24 hours, and the secretion of IL-6 and CXCL8 was determined by ELISA. Compared to the normal-weight non-OA group, synovial fibroblasts from normal-weight OA patients secreted moderately more IL-6 (1.5-fold increase, $P < 0.01$), although there was no difference in the secretion of CXCL8 (Figure 1A). In contrast, the secretion of both IL-6 ($P < 0.001$) and CXCL8 ($P < 0.05$) was markedly elevated in synovial fibroblasts from obese OA patients compared to normal-weight OA and non-OA patients (Figure 1A).

Furthermore, synovial fibroblasts from obese OA patients were more highly proliferative. Thus, fibroblasts from obese OA patients exhibited a more rapid increase in cellular confluence (as determined using IncuCyte cell analysis software) over the first 24 hours following passaging, compared to either normal-weight OA or non-OA patient fibroblasts (Figure 1B). After 7 days of culture, cell numbers of obese OA patient fibroblasts were significantly greater than those of normal-weight OA and non-OA patient fibroblasts, as determined by MTS assay (Figure 1C).

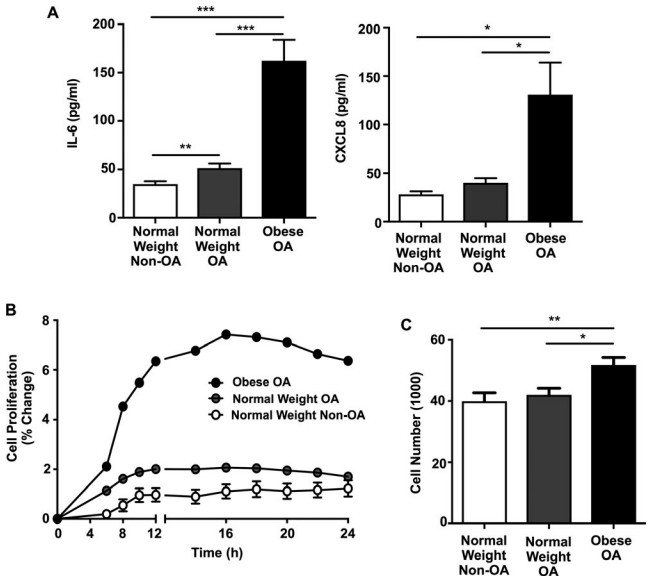

Figure 1. Inflammatory phenotype of synovial fibroblasts from obese patients with hip osteoarthritis (OA). **A**, Protein secretion of interleukin-6 (IL-6) and CXCL8 in primary synovial fibroblasts from normal-weight non-OA, normal-weight OA, and obese OA patients (n = 6 per group), as quantified in culture supernatants by enzyme-linked immunosorbent assay. **B**, Percentage increase in confluency of synovial fibrobasts over 24 hours (n = 3 patients per group), as measured by IncuCyte cell analysis. **C**, Proliferation of synovial fibrobasts after 7 days of culture (n = 3 patients per group), as measured by MTS assay. Results are the mean ± SEM. * = $P < 0.05$, ** = $P < 0.01$; *** = $P < 0.001$, by analysis of variance with Bonferroni's post hoc test.

To further investigate the phenotype of these cells, we next isolated total RNA from the synovial fibroblasts obtained from all 3 patient groups (n = 4 patients per group) and subjected it to 75-bp, paired-end RNA-seq analysis on an Illumina 4000 (performed at the Wellcome Trust Sequencing Unit, University of Oxford, UK). Comparison of the synovial fibroblast expression profile between normal-weight patients with OA and normal-weight non-OA patients identified up-regulation of 344 mRNAs and down-regulation of 606 mRNAs (>2-fold change, $P < 0.05$; change in FPKM >1) (Figures 2A and B, and Supplementary Tables 2 and 3, available on the *Arthritis & Rheumatology* web site at http://onlinelibrary.wiley.com/doi/10.1002/art.41158/abstract). We employed an FPKM cutoff value of >1 based on prior research from the Sequence Quality Control Consortium (31), which showed that this was the level that could be reliably confirmed by qRT-PCR. In addition, our previous studies have shown that lncRNAs and mRNAs have a mean expression level of 2.14 FPKM and 7.03 FPKM, respectively (23) and that cutoffs significantly higher than >1 FPKM would likely preclude large numbers of lncRNAs.

Pathway analysis (using DAVID) of these differentially expressed mRNAs in normal-weight OA patients compared to normal-weight non-OA patients revealed that the top canonical pathways that were associated with the up-regulated genes were the extracellular matrix–receptor interaction and complement/coagulation cascade pathways, whereas among the down-regulated genes, the top associated pathways were those for cell cycle, RNA replication, and cytokine–cytokine interactions (Figure 2C). This was confirmed by IPA, which identified the top pathway as cell cycle control of chromosomal replication, and also identified the top upstream regulator as CDKN2, which encodes 2 proteins (p16 INK4a and p14 arf) that regulate the cell cycle (see Supplementary Tables 4 and 5, available on the *Arthritis & Rheumatology* web site at http://onlinelibrary.wiley.com/doi/10.1002/art.41158/abstract).

Comparison of synovial fibroblasts between normal-weight OA patients and obese OA patients showed that a total of 377 mRNAs were up-regulated and 238 mRNAs were down-regulated (>2-fold change, $P < 0.05$; change in FPKM >1) (Figures 2A and B, and Supplementary Tables 2 and 3 [http://onlinelibrary.wiley.com/doi/10.1002/art.41158/abstract]). In contrast to the comparison between the normal-weight OA and non-OA patient groups, pathway analysis revealed that the most significant up-regulated canonical pathways in obese OA patient fibroblasts were inflammation related, and included cytokine–cytokine interactions, nucleotide-binding oligomerization domain–like receptor signaling, Toll-like receptor signaling, and chemokine signaling pathways (Figure 2C). This inflammatory phenotype was confirmed using IPA (Supplementary Table 4 [http://onlinelibrary.wiley.com/doi/10.1002/art.41158/abstract]).

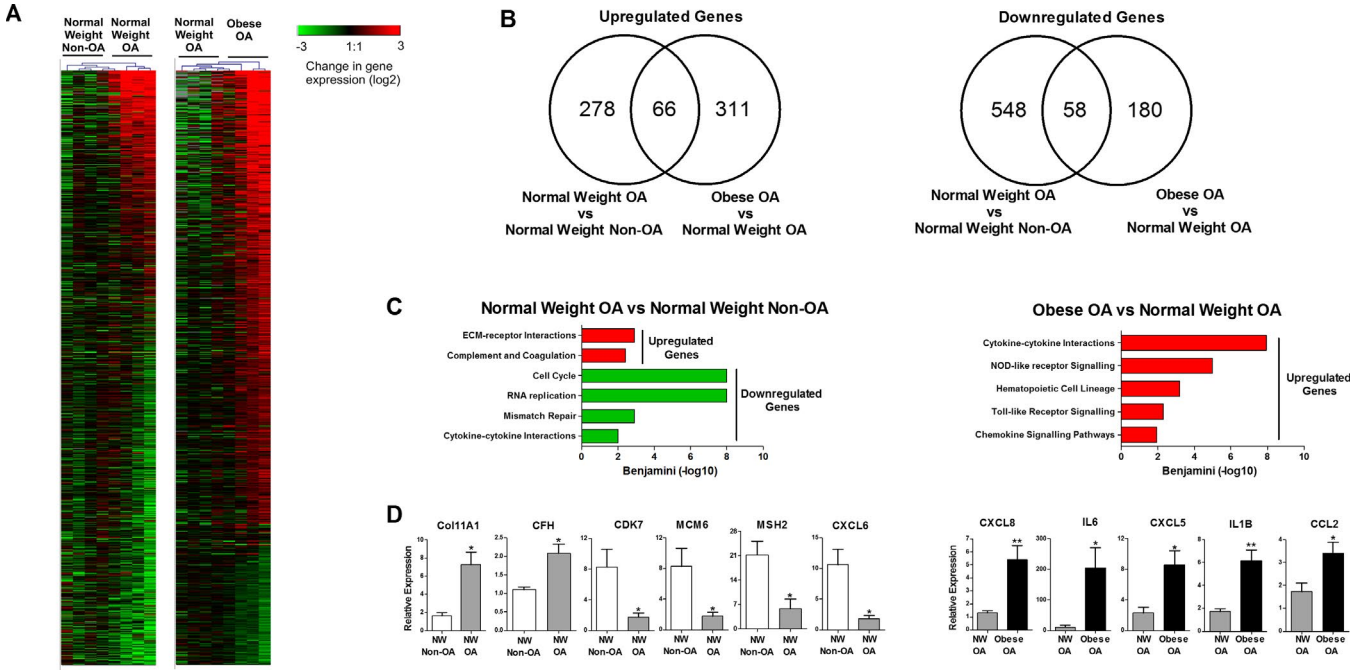

Figure 2. Differentially expressed mRNAs in osteoarthritis (OA) synovial fibroblasts identified using RNA-sequencing (RNA-seq) analysis. **A**, Heatmap showing fold increase in mRNA expression in synovial fibroblasts from normal-weight (NW) non-OA, normal-weight OA, and obese OA patients (n = 4 per group), as determined by RNA-seq. Dendograms were created using the average linkage weighted-pair group method with arithmetic mean. **B**, Venn diagrams of the number of differentially expressed mRNAs (defined as >2-fold change in expression [$P < 0.05$]) and absolute change in expression of >1 fragments per kilobase exon per million reads mapped between normal-weight non-OA and normal-weight OA patient fibroblasts, and between normal-weight OA and obese OA patient fibroblasts. **C**, Top canonical pathways of the differentially expressed mRNAs between normal-weight OA and normal-weight non-OA patient fibroblasts, and between obese OA and normal-weight OA patient fibroblasts, as determined by DAVID pathway analysis. **D**, Differential mRNA expression of genes representing each of the canonical pathways between normal-weight non-OA and normal-weight OA patient fibroblasts (n = 3 per group), and between normal-weight OA and obese OA patient fibroblasts (n = 4 per group), as determined by quantitative reverse transcription–polymerase chain reaction. * = $P < 0.05$; ** = $P < 0.01$. ECM = extracellular matrix; NOD = nucleotide-binding oligomerization domain.

We then selected key representative genes for each of the identified significant canonical pathways and performed qRT-PCR analysis of independent samples to validate the differential expression of each gene between normal-weight non-OA and normal-weight OA patient fibroblasts (n = 3 patients) or between normal-weight OA and obese OA patient fibroblasts (n = 4 patients). The expression of Col11A1 and CFH was confirmed to be significantly up-regulated while the expression of CDK7, MCM6, MSH2, and CXCL6 was confirmed to be significantly down-regulated in fibroblasts from normal-weight OA patients as compared to fibroblasts from normal-weight non-OA patients. The expression of CXCL8, IL6, CXCL5, IL1β, and CCL2 was found to be significantly increased in synovial fibroblasts from obese OA patients as compared to fibroblasts from normal-weight OA patients (Figure 2D).

Identification of lncRNAs associated with the inflammatory phenotype of synovial fibroblasts from obese OA patients. We next analyzed the RNA-seq data to identify lncRNAs that were differentially expressed in synovial fibroblasts between the groups. Initial comparison of normal-weight OA patient fibroblasts and non-OA patient fibroblasts uncovered 19 lncRNAs that were differentially expressed (>2-fold change, $P < 0.05$; change in FPKM >1) (Supplementary Table 6, available on the *Arthritis & Rheumatology* web site at http://onlinelibrary.wiley.com/doi/10.1002/art.41158/abstract). This included 16 long intergenic noncoding RNAs (lincRNAs) and 3 antisense lncRNAs, of which 10 lincRNAs were up-regulated and 6 were down-regulated in normal-weight OA patient fibroblasts compared to normal-weight non-OA patient fibroblasts (Figures 3A and B).

Comparison between synovial fibroblasts from obese OA patients and synovial fibroblasts from normal-weight OA patients identified a total of 19 differentially expressed lncRNAs (Supplementary Table 6 [http://onlinelibrary.wiley.com/doi/10.1002/art.41158/abstract]). Again, this included both antisense and lincRNAs, of which the majority were lincRNAs (15). We observed that 9 lincRNAs were up-regulated and 6 were down-regulated in obese OA patient fibroblasts compared to normal-weight OA patient fibroblasts (Figures 3A and B). Among these lincRNAs, MALAT1 demonstrated the largest absolute increase in expression, rising from 37 FPKM in normal-weight OA to 79 FPKM in obese OA (Supplementary Table 6).

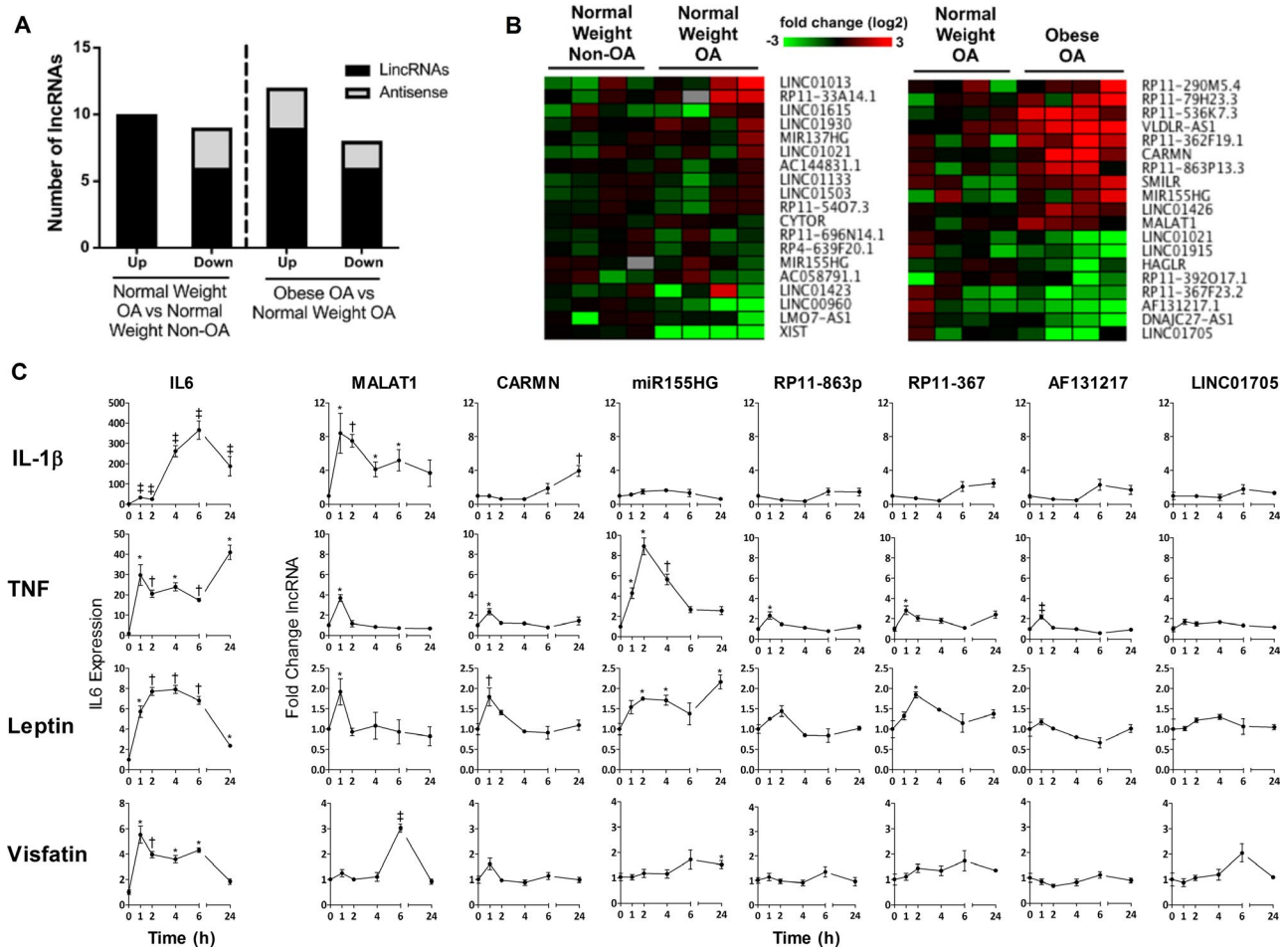

Figure 3. Inflammation-associated long noncoding RNAs (lncRNAs) in osteoarthritis (OA) synovial fibroblasts. **A**, Categorization of the differentially expressed lncRNAs, including antisense and long intergenic noncoding RNAs (lincRNAs), between normal-weight OA and non-OA patient fibroblasts and between obese OA and normal-weight OA patient fibroblasts, as identified by RNA-sequencing. **B**, Heatmaps of differentially expressed lincRNAs in normal-weight non-OA, normal-weight OA, and obese OA patient synovial fibroblasts. **C**, Time course of expression of IL6 mRNA and lincRNAs, as determined by quantitative reverse transcription–polymerase chain reaction in primary human OA synovial fibroblasts over 24 hours following exposure to either interleukin-1β (IL-1β) (1 ng/ml), tumor necrosis factor (TNF) (10 ng/ml), leptin (100 ng/ml), or visfatin (100 ng/ml). Results are the mean ± SEM (n = 3). * = $P < 0.05$; † = $P < 0.01$; ‡ = $P < 0.001$ versus time 0, by analysis of variance with repeated measures. Color figure can be viewed in the online issue, which is available athttp://onlinelibrary.wiley.com/doi/10.1002/art.41158/abstract.

Rapid induction of obesity-associated lincRNAs in response to cytokine stimulation of OA synovial fibroblasts. Of the lincRNAs differentially expressed between normal-weight OA and obese OA synovial fibroblasts, we selected 7 (namely, MALAT1 as well as the lincRNAs CARMN, AF131217.1, miR155HG, LINC01705, RP11-863p13.3, and RP11-367F23.2) and examined their expression in response to an inflammatory challenge. To this end, OA fibroblasts were stimulated with either IL-1β (1 ng/ml), TNF (10 ng/ml), leptin (100 ng/ml), or visfatin (100 ng/ml), and the time course of expression of the 7 lincRNAs and of IL6 mRNA was measured over 24 hours.

As expected, stimulation of OA fibroblasts with either IL-1β, TNF, leptin, or visfatin induced an increase in IL6 mRNA expression (Figure 3C). Examination of lincRNA expression in the OA synovial fibroblasts showed that only the expression of MALAT1 and CARMN were significantly increased in response to stimulation with each of the 4 cytokines, with MALAT1 demonstrating the largest fold changes (Figure 3C). Furthermore, expression of miR155HG increased in response to TNF and leptin, RP11-863p and RP11-367 increased in response to IL-1β, TNF, and leptin, AF131217 increased in response to TNF, and LINC01705 increased in response to visfatin (Figure 3C). Notably, we found that the synovial fluid cytokine concentrations of TNF ($P < 0.01$) and leptin ($P < 0.05$) were significantly elevated in obese OA patients compared to normal-weight OA patients, and both were significantly correlated with the expression of MALAT1, IL6, and CXCL8 in obese OA patients (see Supplementary Figure 1, available on the *Arthritis & Rheumatology* web site at http://onlinelibrary.wiley.com/doi/10.1002/art.41158/abstract). The level of IL-1β was also elevated in synovial fluid from obese OA patients com-

pared to normal-weight OA patients, although this difference did not reach statistical significance ($P = 0.07$). Nevertheless, IL-1β synovial fluid concentrations were significantly correlated with the expression of MALAT1 ($P < 0.01$) (Supplementary Figure 1). Given that MALAT1 showed both the largest absolute change in expression between normal-weight OA and obese OA patient fibroblasts and was ubiquitously induced (with the largest fold changes) in response to inflammatory mediators, subsequent studies were focused on elucidating the in vivo relevance and function of MALAT1.

Differential expression of MALAT1 in inflammatory OA synovial tissue. To examine the potential in vivo relevance of MALAT1, we extracted total RNA from the synovium of normal-weight non-OA patients (n = 6), normal-weight OA patients (n = 8), and obese OA patients (n = 8). Expression of MALAT1 was significantly up-regulated in normal-weight OA patient synovium compared to normal-weight non-OA patient synovium, and was further increased in obese OA patient synovium (Figure 4A). Interestingly, down-regulation of MALAT1 mRNA expression was associated with increased expression of the inflammatory genes IL6 and CXCL8 (Figure 4A).

Regulation of the inflammatory response and cell proliferation by MALAT1 in fibroblasts from obese OA patients. Subsequently, we undertook knockdown studies to ascertain whether changes in MALAT1 expression could be causally linked to the increased inflammatory and proliferative response of synovial fibroblasts from obese OA patients. To this end, fibroblasts from obese OA patients were transfected with 2 different LNA GapmeRs targeting MALAT1 or with a nontargeting control LNA (each at 30 n*M*; Exiqon). Both MALAT1 LNAs produced a >90% knockdown in expression of MALAT1 mRNA after 24 hours, compared to cells transfected with the nontargeting control LNA (Figure 4B). Fibroblasts depleted of MALAT1 expressed significantly reduced levels of CXCL8 mRNA and CXCL8 protein secretion (Figure 4C). Furthermore, fibroblasts depleted of MALAT1 also displayed significantly reduced cellular proliferation as compared to fibroblasts transfected with control LNA, both at 48 hours and after 5 days of culture (Figure 4D).

To further investigate the role of MALAT1 on the OA synovial fibroblast transcriptome, we then performed an additional MALAT1 loss-of-function study. To this end, OA synovial fibroblasts (n = 4 patients) were transfected for 24 hours with 1 of 2 different LNA GapmeRs targeting MALAT1 or with a nontargeting control LNA (each at 30 n*M*; Exiqon), and total RNA was subjected to RNA-seq analysis (Lexogen).

In total, RNA-seq identified 28 mRNAs, including CXCL8 mRNA, that were differentially expressed (>1.5 fold, $P < 0.05$) following MALAT1 knockdown, with comparable findings yielded by both MALAT1 LNA GapmeRs (Figures 5A and B, and Supplementary Tables 7 and 8, available on the *Arthritis & Rheumatology* web site at http://onlinelibrary.wiley.com/doi/10.1002/art.41158/abstract).

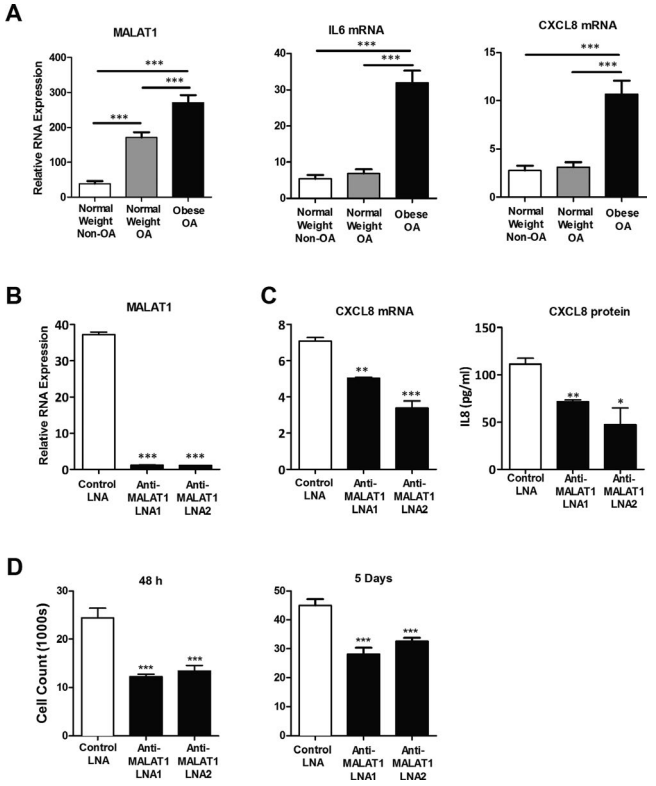

Figure 4. Expression and functional role of the long noncoding RNA (lncRNA) for metastasis-associated lung adenocarcinoma transcript 1 (MALAT1) in osteoarthritis (OA) synovial tissue. **A**, Differential expression of MALAT1 lncRNA and inflammatory IL6 and CXCL8 mRNAs in normal-weight non-OA (n = 6), normal-weight OA (n = 8), and obese OA (n = 8) patient synovial tissue. Expression was determined by quantitative reverse transcription–polymerase chain reaction (qRT-PCR), with values normalized to the values for 18S. * = $P < 0.05$; ** = $P < 0.01$; *** = $P < 0.001$, by analysis of variance (ANOVA) with Bonferroni's post hoc test. **B**, LNA-mediated knockdown of MALAT1 in OA synovial fibroblasts. Synovial fibroblasts were transfected for 24 hours with either a control LNA or 2 different MALAT1 LNA GapmeRs. MALAT1 knockdown was determined by qRT-PCR, with values normalized to the values for 18S. **C**, Effect of LNA-mediated MALAT1 knockdown using 2 different MALAT1 LNA GapmerRs on the expression of CXCL8 mRNA and secretion of CXCL8 protein in OA fibroblasts (n = 4 patients). Expression of mRNA was determined by qRT-PCR, with values normalized to the values for 18S. CXCL8 protein was measured by enzyme-linked immunosorbent assay. In **B** and **C**, * = $P < 0.05$; ** = $P < 0.01$; *** = $P < 0.001$ versus control LNA–transfected fibroblasts, by ANOVA with Dunnett's post hoc test. **D**, Effect of LNA-mediated knockdown of MALAT1 on the proliferation of OA synovial fibroblasts 48 hours and 5 days posttransfection, as determined by MTS assay. *** = $P < 0.001$ versus control LNA–transfected fibroblasts, by ANOVA. Results are the mean ± SEM.

The effect of MALAT1 knockdown on the differential expression of the mRNAs for CXCL8, TRIM6, IL7R, HIST1H1C, and MAML3 was then validated by qRT-PCR, and a significant correlation in the fold change data was observed between the RNA-seq

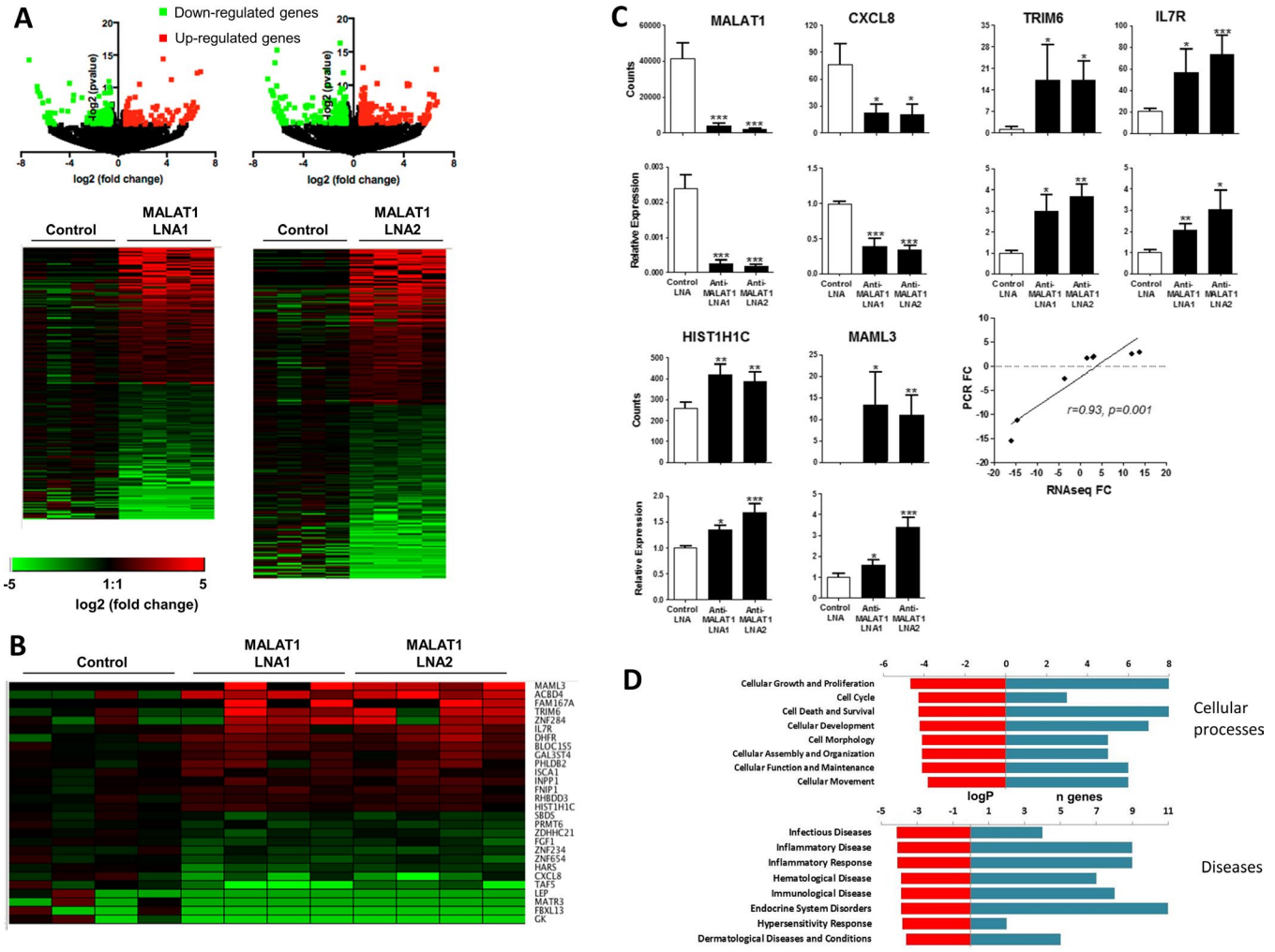

Figure 5. RNA-sequencing (RNA-seq) analysis of the effects of knockdown of the metastasis-associated lung adenocarcinoma transcript 1 (MALAT1) long noncoding RNA in OA synovial fibroblasts. **A**, Volcano plots and heatmaps of RNA-seq data showing fold change (FC) in the differentially expressed mRNAs (fold change >1.5, $P < 0.05$) after knockdown with either MALAT1 LNA1 or MALAT1 LNA2 GapmeRs compared to control LNA (n = 4 patients per group). **B**, Heatmap of expression of mRNAs for the 28 differentially expressed genes (fold change >1.5, $P < 0.05$), following knockdown with the MALAT1 GapmeRs compared to control LNA. **C**, Comparison of RNA-seq counts with quantitative reverse transcription–polymerase chain reaction (qRT-PCR) relative expression data for the MALAT1, CXCL8, TRIM6, IL7R, HIST1H1c, and MAML3 genes, and Pearson's analysis of correlation between the PCR fold change data and RNA-seq fold change data. Results are the mean ± SEM. * = $P < 0.05$; ** = $P < 0.01$; *** = $P < 0.001$ versus control LNA–transfected fibroblasts, by analysis of variance with Dunnett's post hoc test. **D**, Top cellular processes and disease functions as determined by Ingenuity Pathway Analysis of the differentially expressed mRNAs (fold change >1.5, $P < 0.05$) following MALAT1 knockdown. Color figure can be viewed in the online issue, which is available athttp://onlinelibrary.wiley.com/doi/10.1002/art.41158/abstract.

and qRT-PCR analyses (r = 0.93, $P = 0.001$) (Figure 5C). Further investigation using pathway analysis of the 28 differential mRNAs revealed that the most significantly affected cellular processes included those for cellular growth and proliferation, while the most significantly affected disease functions included inflammatory response and inflammatory disorders (Figure 5D).

DISCUSSION

The role of synovitis as a disease driver in OA has been largely understudied, with OA tissue often being used as a noninflammatory control in comparative studies of patients with rheumatoid arthritis. Importantly, in the present study we demonstrate, for the first time, that synovial fibroblasts isolated from the synovium of patients with hip OA exhibit a more inflammatory and proliferative phenotype in those patients who are obese, compared to normal-weight OA patients.

Synovial fibroblasts from obese OA patients secreted greater protein amounts of IL-6 and CXCL8 than did synovial fibroblasts from normal-weight OA patients. Notably, OA disease processes in the absence of obesity had little effect on the inflammatory phenotype of the synovial tissue. For example, synovial tissue mRNA

expression and protein secretion of CXCL8 from isolated synovial fibroblasts did not differ between normal-weight OA patients and normal-weight patients without OA. Likewise, there was no difference in the synovial tissue expression of IL-6 between non-OA and OA patients of normal weight, and only a small increase in IL-6 secretion in synovial fibroblasts from normal-weight OA patients compared to synovial fibroblasts from non-OA patients. Furthermore, the proliferative activity of fibroblasts was similar between non-OA and normal-weight OA.

Transcriptomics analysis of synovial fibroblasts revealed that obese OA patient synovial fibroblasts exhibited differential expression of a plethora of inflammatory mRNAs (including cytokines, chemokines, and their receptors), compared to normal-weight OA patient fibroblasts. Pathway analysis of these differentially expressed mRNAs predicted a significant role of activation chemokine signaling pathways.

These findings may have important implications for patient stratification. Clinical trials of antiinflammatory therapies in OA have produced disappointing results (3). Adalimumab, a TNF-neutralizing antibody, was deemed ineffective at reducing disease activity in patients with erosive hand OA (32). Similarly, treatment of knee OA patients with AMG108, an IL-1β receptor–neutralizing antibody, failed to significantly reduce pain (33). However, these trials did not select patients based on their degree of synovial inflammation. Notably, in a clinical trial of the effectiveness of adalimumab to alleviate knee pain in OA, 40% of patients had a 50% improvement in their pain score (34). Our data would suggest that the degree of synovial inflammation in the patients recruited for these studies would have been dependent on their body mass index. Given our findings, it would be pertinent to consider whether those patients who responded were obese and exhibited greater synovial inflammation.

In addition to coding genes, our study has identified several lncRNAs that are differentially expressed in OA patient fibroblasts compared to non-OA patient fibroblasts, as well as lncRNAs that are differentially expressed in obese OA patient fibroblasts compared to normal-weight OA patient fibroblasts. Given the potential clinical implications of the inflammatory phenotype of synovial fibroblasts in obese patients with OA, it was notable that the majority of the differentially expressed lncRNAs were classified as lincRNAs. Evidence has emerged to indicate that lincRNAs are central regulators of the inflammatory response in multiple cell types. Indeed, we recently identified lincRNAs associated with the human OA chondrocyte inflammatory response, which were induced in response to an inflammatory challenge and functioned to mediate the production of IL-6 (22).

In the present study we found that the expression of obesity-associated lincRNAs in synovial fibroblasts was modulated by stimulation with proinflammatory cytokines and adipokines. Of the lincRNAs investigated, MALAT1 was the most responsive to proinflammatory challenge, being rapidly induced following stimulation of synovial fibroblasts. This induction was transient, with MALAT1 expression returning to baseline levels within 24 hours, and occurred prior to an increase in the expression of IL6 and CXCL8 mRNA. Such rapid and transient expression in response to an inflammatory challenge is indicative of MALAT1 being an important regulator of synovial fibroblast inflammation, which is supported by our finding that depletion of MALAT1 from obese OA patient synovial fibroblasts reduced the expression and secretion of CXCL8, and globally had an impact on mRNAs that regulate cellular growth and proliferation and the inflammatory response, including IL7R, TRIM6, HIST1H1C, and MAML3. There is precedent for a role of MALAT1 as a regulator of inflammation, including the regulation of CXCL8. In hepatocellular carcinoma cells, MALAT1 knockdown decreased the expression of CXCL8 and IL-6 (35). In human endothelial cells, depletion of MALAT1 with small interfering RNA (siRNA) reduced the expression of TNF and IL-6 (36,37), while MALAT1 knockdown in monocytes from patients with systemic lupus erythematosus reduced the expression of IL-21 (38). In vivo, inflammation markers, including IL-6, IL-1β, TNF, and interferon-γ, were all supressed in MALAT1-knockout diabetic mice compared to wild-type mice (36). Mechanistically, MALAT1 has recently been reported to bind to and modulate NF-κB activity, thereby regulating the lipopolysaccharide-induced inflammatory response (39,40).

We also found that depletion of MALAT1 reduced the proliferation of synovial fibroblasts from obese OA patients, suggesting that targeted inhibition of MALAT1 in the synovial joint could have the dual action of reducing both synovial inflammation and hyperplasia. Several studies using cancer cell models have demonstrated that MALAT1 is a regulator of cellular proliferation. Knockdown of MALAT1 by siRNA in non–small cell lung cancer A549 cells inhibited their proliferation both in vitro and in a xenograft tumor growth model (41). Similarly, knockdown of MALAT1 inhibited the proliferation of the human triple-negative breast cancer cell line MDA-MB-453 (42).

It is important to note that our study only examined the synovium from patients with hip OA. Similar to the knee, the hip is a weight-bearing joint. Therefore, the obesity-associated inflammatory synovial fibroblast phenotype described herein may be initiated and promoted by excess loading on the joint. However, obesity is associated with OA in both weight-bearing and non–weight-bearing joints, supporting the notion that the effect of obesity is not simply attributable to increased joint loading. Indeed, it is known that obesity is associated with increased circulatory levels of proinflammatory cytokines and adipokines (43,44). We previously reported that the adipokine resistin is elevated systemically and more highly expressed in the synovial joint tissue in obese patients with hip OA as compared to normal-weight patients with hip OA (45), and it was recently found that patients with hand OA exhibit increased circulatory levels of resistin (46). Thus, the obesity-associated inflammatory synovial fibroblast phenotype may be replicated in non–weight-bearing OA joints.

In summary, these data demonstrate that obesity in OA patients is associated with an inflammatory synovial fibroblast

phenotype, and further supports the notion that lncRNAs, and in particular MALAT1, are central regulators of the inflammatory response in the OA synovial joint. Determining the effect of obesity on the inflammatory phenotype of synovial tissue in both weight-bearing and non–weight-bearing joints and the relationship to the expression and functional role of lncRNAs will provide new insights into our understanding of how OA joint inflammation is regulated, and may lead to the development of novel antiinflammatory disease-modifying therapies or to the repurposing of existing therapies for OA.

ACKNOWLEDGMENTS

The authors would like to acknowledge all study participants and also the research staff at The Royal Orthopaedic Hospital NHS Foundation Trust (Birmingham, UK), Russell's Hall Hospital (Dudley, UK), and Kings Mill Hospital (Sutton in Ashfield, UK) for obtaining informed consent and performing patient screenings. In addition, the authors acknowledge the contributions of the orthopaedic surgeons David Dunlop, Matthew Revell, and Sohail Quraishi.

AUTHOR CONTRIBUTIONS

All authors were involved in drafting the article or revising it critically for important intellectual content, and all authors approved the final version to be published. Dr. Jones had full access to all of the data in the study and takes responsibility for the integrity of the data and the accuracy of the data analysis.

Study conception and design. Lindsay, Jones.

Acquisition of data. Nanus, Wijesinghe, Pearson, Hadjicharalambous, Rosser, Davis, Lindsay, Jones.

Analysis and interpretation of data. Lindsay, Jones.

REFERENCES

1. Ganesan R, Rasool M. Fibroblast-like synoviocytes-dependent effector molecules as a critical mediator for rheumatoid arthritis: current status and future directions [review]. Int Rev Immunol 2017;36:20–30.
2. Tonge DP, Pearson MJ, Jones SW. The hallmarks of osteoarthritis and the potential to develop personalised disease-modifying pharmacological therapeutics. Osteoarthritis Cartilage 2014;22: 609–21.
3. Philp AM, Davis ET, Jones SW. Developing anti-inflammatory therapeutics for patients with osteoarthritis. Rheumatology (Oxford) 2017;56:869–81.
4. Mathiessen A, Conaghan PG. Synovitis in osteoarthritis: current understanding with therapeutic implications [review]. Arthritis Res Ther 2017;19:18.
5. Jones SW, Brockbank SM, Clements KM, Le Good N, Campbell D, Read SJ, et al. Mitogen-activated protein kinase-activated protein kinase 2 (MK2) modulates key biological pathways associated with OA disease pathology. Osteoarthritis Cartilage 2009;17: 124–31.
6. Brown KK, Heitmeyer SA, Hookfin EB, Hsieh L, Buchalova M, Taiwo YO, et al. P38 MAP kinase inhibitors as potential therapeutics for the treatment of joint degeneration and pain associated with osteoarthritis. J Inflamm (Lond) 2008;5:22.
7. Kapoor M, Martel-Pelletier J, Lajeunesse D, Pelletier JP, Fahmi H. Role of proinflammatory cytokines in the pathophysiology of osteoarthritis. Nat Rev Rheumatol 2011;7:33–42.
8. Fernandez-Madrid F, Karvonen RL, Teitge RA, Miller PR, An T, Negendank WG. Synovial thickening detected by MR imaging in osteoarthritis of the knee confirmed by biopsy as synovitis. Magn Reson Imaging 1995;13:177–83.
9. Oehler S, Neureiter D, Meyer-Scholten C, Aigner T. Subtyping of osteoarthritic synoviopathy. Clin Exp Rheumatol 2002;20:633–40.
10. Rhodes LA, Conaghan PG, Radjenovic A, Grainger AJ, Emery P, McGonagle D. Further evidence that a cartilage-pannus junction synovitis predilection is not a specific feature of rheumatoid arthritis. Ann Rheum Dis 2005;64:1347–9.
11. Myers SL, Brandt KD, Ehlich JW, Braunstein EM, Shelbourne KD, Heck DA, et al. Synovial inflammation in patients with early osteoarthritis of the knee. J Rheumatol 1990;17:1662–9.
12. Korkusuz P, Dagdeviren A, Eksioglu F, Ors U. Immunohistological analysis of normal and osteoarthritic human synovial tissue. Bull Hosp Jt Dis 2005;63:63–9.
13. De Lange-Brokaar BJ, Ioan-Facsinay A, van Osch GJ, Zuurmond AM, Schoones J, Toes RE, et al. Synovial inflammation, immune cells and their cytokines in osteoarthritis: a review. Osteoarthritis Cartilage 2012;20:1484–99.
14. Revell PA, Mayston V, Lalor P, Mapp P. The synovial membrane in osteoarthritis: a histological study including the characterisation of the cellular infiltrate present in inflammatory osteoarthritis using monoclonal antibodies. Ann Rheum Dis 1988;47:300–7.
15. Pearson MJ, Herndler-Brandstetter D, Tariq MA, Nicholson TA, Philp AM, Smith HL, et al. IL-6 secretion in osteoarthritis patients is mediated by chondrocyte-synovial fibroblast cross-talk and is enhanced by obesity. Sci Rep 2017;7:3451.
16. Deleuran B, Lemche P, Kristensen M, Chu CQ, Field M, Jensen J, et al. Localisation of interleukin 8 in the synovial membrane, cartilage-pannus junction and chondrocytes in rheumatoid arthritis. Scand J Rheumatol 1994;23:2–7.
17. Hulejová H, Baresová V, Klézl Z, Polanská M, Adam M, Senolt L. Increased level of cytokines and matrix metalloproteinases in osteoarthritic subchondral bone. Cytokine 2007;38:151–6.
18. Cabili MN, Trapnell C, Goff L, Koziol M, Tazon-Vega B, Regev A, et al. Integrative annotation of human large intergenic noncoding RNAs reveals global properties and specific subclasses. Genes Dev 2011;25:1915–27.
19. Mercer TR, Gerhardt DJ, Dinger ME, Crawford J, Trapnell C, Jeddeloh JA, et al. Targeted RNA sequencing reveals the deep complexity of the human transcriptome. Nat Biotechnol 2011;30:99–104.
20. Austin PJ, Tsitsiou E, Boardman C, Jones SW, Lindsay MA, Adcock IM, et al. Transcriptional profiling identifies the long noncoding RNA plasmacytoma variant translocation (PVT1) as a novel regulator of the asthmatic phenotype in human airway smooth muscle. J Allergy Clin Immunol 2017;139:780–9.
21. Pearson MJ, Jones SW. Long noncoding RNAs in the regulation of inflammatory pathways in rheumatoid arthritis and osteoarthritis [review]. Arthritis Rheumatol 2016;68:2575–83.
22. Pearson MJ, Philp AM, Heward JA, Roux BT, Walsh DA, Davis ET, et al. Long intergenic noncoding RNAs mediate the human chondrocyte inflammatory response and are differentially expressed in osteoarthritis cartilage. Arthritis Rheumatol 2016;68:845–56.
23. Ilott NE, Heward JA, Roux B, Tsitsiou E, Fenwick PS, Lenzi L, et al. Corrigendum: long non-coding RNAs and enhancer RNAs regulate the lipopolysaccharide-induced inflammatory response in human monocytes. Nat Commun 2015;6:6814.
24. Hamann PD, Roux BT, Heward JA, Love S, McHugh NJ, Jones SW, et al. Transcriptional profiling identifies differential expression of long non-coding RNAs in Jo-1 associated and inclusion body myositis. Sci Rep 2017;7:8024.

25. Roux BT, Heward JA, Donnelly LE, Jones SW, Lindsay MA. Catalog of differentially expressed long non-coding RNA following activation of human and mouse innate immune response. Front Immunol 2017;8:1038.
26. Pertea M, Kim D, Pertea GM, Leek JT, Salzberg SL. Transcript-level expression analysis of RNA-seq experiments with HISAT, StringTie and Ballgown. Nat Protoc 2016;11:1650–67.
27. Li H, Handsaker B, Wysoker A, Fennell T, Ruan J, Homer N, et al. The Sequence Alignment/Map format and SAMtools. Bioinformatics 2009;25:2078–9.
28. Pertea M, Pertea GM, Antonescu CM, Chang TC, Mendell JT, Salzberg SL. StringTie enables improved reconstruction of a transcriptome from RNA-seq reads. Nat Biotechnol 2015;33:290–5.
29. Trapnell C, Williams BA, Pertea G, Mortazavi A, Kwan G, van Baren MJ, et al. Transcript assembly and quantification by RNA-Seq reveals unannotated transcripts and isoform switching during cell differentiation. Nat Biotechnol 2010;28:511–5.
30. Sturn A, Quackenbush J, Trajanoski Z. Genesis: cluster analysis of microarray data. Bioinformatics 2002;18:207–8.
31. SEQC/MAQC-III Consortium. A comprehensive assessment of RNA-seq accuracy, reproducibility and information content by the Sequencing Quality Control Consortium. Nat Biotechnol 2014;32:903–14.
32. Verbruggen G, Wittoek R, Vander Cruyssen B, Elewaut D. Tumour necrosis factor blockade for the treatment of erosive osteoarthritis of the interphalangeal finger joints: a double blind, randomised trial on structure modification. Ann Rheum Dis 2012;71:891–8.
33. Cohen SB, Proudman S, Kivitz AJ, Burch FX, Donohue JP, Burstein D, et al. A randomized, double-blind study of AMG 108 (a fully human monoclonal antibody to IL-1R1) in patients with osteoarthritis of the knee. Arthritis Res Ther 2011;13:R125.
34. Maksymowych WP, Russell AS, Chiu P, Yan A, Jones N, Clare T, et al. Targeting tumour necrosis factor alleviates signs and symptoms of inflammatory osteoarthritis of the knee. Arthritis Res Ther 2012;14:R206.
35. Huang M, Wang H, Hu X, Cao X. lncRNA MALAT1 binds chromatin remodeling subunit BRG1 to epigenetically promote inflammation-related hepatocellular carcinoma progression. Oncoimmunology 2018;8:e1518628.
36. Biswas S, Thomas AA, Chen S, Aref-Eshghi E, Feng B, Gonder J, et al. MALAT1: an epigenetic regulator of inflammation in diabetic retinopathy. Sci Rep 2018;8:6526.
37. Puthanveetil P, Chen S, Feng B, Gautam A, Chakrabarti S. Long non-coding RNA MALAT1 regulates hyperglycaemia induced inflammatory process in the endothelial cells. J Cell Mol Med 2015;19:1418–25.
38. Yang H, Liang N, Wang M, Fei Y, Sun J, Li Z, et al. Long noncoding RNA MALAT-1 is a novel inflammatory regulator in human systemic lupus erythematosus. Oncotarget 2017;8:77400–6.
39. Zhao G, Su Z, Song D, Mao Y, Mao X. The long noncoding RNA MALAT1 regulates the lipopolysaccharide-induced inflammatory response through its interaction with NF-κB. FEBS Lett 2016;590:2884–95.
40. Zhou HJ, Wang LQ, Wang DB, Yu JB, Zhu Y, Xu QS, et al. Long noncoding RNA MALAT1 contributes to inflammatory response of microglia following spinal cord injury via the modulation of a miR-199b/IKKβ/NF-κB signaling pathway. Am J Physiol Cell Physiol 2018;315:C52–61.
41. Ma J, Wu K, Liu K, Miao R. Effects of MALAT1 on proliferation and apoptosis of human non-small cell lung cancer A549 cells in vitro and tumor xenograft growth in vivo by modulating autophagy. Cancer Biomark 2018;22:63–72.
42. Zuo Y, Li Y, Zhou Z, Ma M, Fu K. Long non-coding RNA MALAT1 promotes proliferation and invasion via targeting miR-129-5p in triple-negative breast cancer. Biomed Pharmacother 2017;95:922–8.
43. Ellulu MS, Patimah I, Khaza'ai H, Rahmat A, Abed Y. Obesity and inflammation: the linking mechanism and the complications. Arch Med Sci 2017;13:851–63.
44. Scherer PE. Adipose tissue: from lipid storage compartment to endocrine organ. Diabetes 2006;55:1537–45.
45. Philp AM, Collier RL, Grover LM, Davis ET, Jones SW. Resistin promotes the abnormal type I collagen phenotype of subchondral bone in obese patients with end stage hip osteoarthritis. Sci Rep 2017;7:4042.
46. Fioravanti A, Cheleschi S, De Palma A, Addimanda O, Mancarella L, Pignotti E, et al. Can adipokines serum levels be used as biomarkers of hand osteoarthritis? Biomarkers 2018;23:265–70.